JOURNAL OF BACTERIOLOGY, Nov. 1994, p. 7121–7125
0021-9193/94/$04.00+0

Vol. 176, No. 22

Comparative Genome Mapping with Mobile Physical Map Landmarks

CRAIG A. BLOCH,[1,2]* CHRISTOPHER K. RODE,[1] VICTOR OBREQUE,[1] AND KELLY Y. RUSSELL[1]

Department of Pediatrics, School of Medicine,[1] and Department of Epidemiology, School of Public Health,[2] University of Michigan, Ann Arbor, Michigan 48109

Received 10 February 1994/Accepted 9 September 1994

We describe a method for comparative macrorestriction mapping of the chromosomes of *Escherichia coli* strains. In this method, a series of physically tagged *E. coli* K-12 alleles serve as mobile landmarks for mapping DNAs from other strains. This technique revealed evidence of strain-specific chromosomal additions or deletions in a pathogenic isolate and can be applied to most strains, yielding information on genealogy as well as virulence. In theory, the same strategy can be used to map and compare genomic DNAs from a wide variety of species.

Application of physical mapping techniques for comparing evolutionarily diverged *Escherichia coli* chromosomes is typically not straightforward. For instance, use of Southern analysis to align the chromosomal restriction fragments of diverged strains may yield conflicting data as a result of sequence repeats (17). Recently, bacteriophage P1 transduction of alleles tagged by transposon insertions has been used to align corresponding chromosomal *Not*I (10) and *Sfi*I (18) restriction fragments from pairs of *E. coli* K-12 strains. Aligning chromosomal fragments by this procedure is not usually subject to the limitations encountered with standard physical mapping techniques because it depends, in part, on genetic detection of shared homologies. We reasoned that, similarly, genetic inference could be adapted for identification of physical map alignments between the chromosomes of even substantially more diverged *E. coli* isolates. This report demonstrates use of K-12 alleles bearing insertions of the recognition site for the rare-cutting restriction endonuclease *Not*I to construct a comparative macrorestriction map of the chromosomes of *E. coli* K-12 and a pathogenic *E. coli* strain.

(Preliminary results of this work were presented previously [23].)

The *E. coli* strains and phages and plasmids used in this study are listed in Table 1. A series of nine *E. coli* K-12 transposon insertions linked to known markers between 63 and 86 min was isolated by P1 cotransduction (15). The pooled inserts from which this series was isolated were generated in K-12 strain MG1655 (1) through combined use of an altered-target-specificity IS*10* transposase (3) and minitransposon 'Tn*10*dKanRCP1' (13) containing a transposase deletion and the *Not*I restriction enzyme recognition site. (The corresponding insertion mutants were generated by electroporation [8] of strain MG1655 with suicide plasmid pGI250 DNA [13].) The genetic map coordinates of each of these nine MG1655 chromosomal Tn*10*dKanRCP1 inserts were confirmed through cotransductional linkage analyses to flanking K-12 markers (28) (results not shown).

The nine corresponding MG1655::Tn*10*dKanRCP1 alleles could be mobilized not only into K-12-derived strains, but also into other *E. coli* backgrounds. These alleles were introduced into wild-type strain MG1655 and neonatal meningitis-associated strain RS218 (5) by P1 transduction (15). Transductants from all crosses arose at frequencies of $\sim 10^{-6}$ CFU per recipient and formed grossly normal colonies on solid Luria-Bertani medium (15). For each cross, *Not*I digestion and pulsed-field gel electrophoresis of genomic DNAs, which were carried out as described elsewhere (10), confirmed a uniform integration site in multiple transductants (results not shown).

Changes in the *Not*I digestion patterns of DNAs from pairs of MG1655 and RS218 transductants, each pair having inherited the same Tn*10*dKanRCP1 insert, are shown in Table 2. Incorporation of an insert in either strain resulted in the loss of a single native *Not*I fragment and the appearance of two smaller subfragments. From such data, the location of an insert could be narrowed to two possible positions relative to the preexisting *Not*I sites flanking it (see reference 19 for a detailed example). Its location could then be further narrowed to only one position from the alterations caused by additional inserts at neighboring linkage map coordinates contained between the same two preexisting *Not*I sites; these indicated the clockwise and counterclockwise distances from the flanking sites to the insert and, thereby, its precise physical map coordinate (disregarding the asymmetry of the *Not*I site in the 1.2-kb Tn*10*dKanRCP1 element).

A comparison of the size discrepancies among fragments created by the insertion of Tn*10*dKanRCP1 at different positions in the same native MG1655 *Not*I fragment (either fragment A or fragment L) confirmed the orientations of the subfragments predicted from the *E. coli* linkage map and the MG1655 *Not*I map (Table 2 [χM1346, χM1347, χM1348, χM1349, χM1350, and χM1352 or χM1353, χM1354, and χM1355]). When the same insertions were transduced into strain RS218, the changes in the *Not*I digestion patterns made it possible to align several RS218 *Not*I fragments with the linkage map; these data indicated that fragment A of strain RS218 contains ~61 to ~81 min (Table 2 [χM1501 to χM1506]) and that fragment K of strain RS218 contains ~81 to ~86 min and corresponds to fragment L of strain MG1655 (Table 2 [χM1507 to χM1509]).

While it is possible that pairs of corresponding Tn*10*d KanRCP1 inserts in strains MG1655 and RS218 would reveal regional chromosomal size identities or discrepancies between the two strains, many of these might be obscured in restriction

* Corresponding author. Mailing address: Medical Science Research Building I, Room A500, 1150 West Medical Center Drive, Ann Arbor, MI 48109-0656. Fax: (313) 764-6837. Electronic mail address: Craig.Bloch@UM.cc.UMich.edu.

TABLE 1. Strains, phages, and plasmids used in this study

Strain, phage, or plasmid	Description	Source and/or reference
E. coli laboratory strains		
MG1655	K-12 prototype; F^- λ^- Mal^+ Tc^s Km^s Cm^s	B. Eisenstein (9)
GE2515	MG1655/pMS421/pJD12; delivery system for Tn*10*dCamMCS; *tac* promoter-inducible transposase; Cm^r	G. Weinstock (10)
CAG12177	MG1655 *zeh-298*::Tn*10*;Tc^r	R. Matthews (28)
CAG12168	MG1655 *zgd-210*::Tn*10*;Tc^r	R. Matthews (28)
CAG18475	MG1655 *metC162*::Tn*10*;Tc^r	R. Matthews (28)
CAG12152	MG1655 *zgh-3075*::Tn*10*;Tc^r	R. Matthews (28)
CAG12153	MG1655 *zha-6*::Tn*10*;Tc^r	R. Matthews (28)
CAG12075	MG1655 *zhd-3083*::Tn*10*;Tc^r	R. Matthews (28)
P678	*thr-1 ara-13 leuB6 tonA2 lacY1 supE44 gal-6 rfbD1 galP63 malT1* λ^r *xyl-7 mtlA2 thi-1* Cm^s	I. Blomfield (1)
CAG18501	MG1655 *zie-296*::Tn*10*;Tc^r	R. Matthews (28)
CAG18431	MG1655 *ilv-500*::Tn*10*;Tc^r	R. Matthews (28)
χM1337	CAG12168 *zgd-1*::Tn*10*dKanRCP1;Tc^s Km^r	This study
χM1338	CAG18475 *zgf-1*::Tn*10*dKanRCP1;Tc^s Km^r	This study
χM1339	CAG12152 *zgh-1*::Tn*10*dKanRCP1;Tc^s Km^r	This study
χM1340	CAG12153 *zha-1*::Tn*10*dKanRCP1;Tc^s Km^r	This study
χM1341	CAG12075 *zhd-1*::Tn*10*dKanRCP1;Tc^s Km^r	This study
χM1342[a]	P678 *zhf-2*::Tn*10*dCamMCS;Mal^+ Cm^r	This study
χM1343	CAG12177 (Tn*10*dKanRCP1);Tc^s Km^r; P1 donor to generate χM1353	This study
χM1344	CAG18501 *zie-1*::Tn*10*dKanRCP1;Tc^s Km^r	This study
χM1345	CAG18431 *zif-1*::Tn*10*dKanRCP1;Tc^s Km^r	This study
χM1346	MG1655 *zgd-1*::Tn*10*dKanRCP1;Km^r	This study
χM1347	MG1655 *zgf-1*::Tn*10*dKanRCP1;Km^r	This study
χM1348	MG1655 *zgh-1*::Tn*10*dKanRCP1;Km^r	This study
χM1349	MG1655 *zha-1*::Tn*10*dKanRCP1;Km^r	This study
χM1350	MG1655 *zhd-1*::Tn*10*dKanRCP1;Km^r	This study
χM1352	MG1655 *zhf-2*::Tn*10*dCamMCS;Cm^r	This study
χM1353	MG1655 *zid-1*::Tn*10*dKanRCP1;Km^r	This study
χM1354	MG1655 *zie-1*::Tn*10*dKanRCP1;Km^r	This study
χM1355	MG1655 *zif-1*::Tn*10*dKanRCP1;Km^r	This study
E. coli pathogenic strain		
RS218	Serotype O18:K1:H7; newborn-meningitis prototype; Km^s Cm^s	R. Silver (27)
E. coli RS218–K-12 chimeras		
χM1500	RS218 *zfj-1*::Tn*10*dKanRCP1;Km^r	This study
χM1501	RS218 *zgd-1*::Tn*10*dKanRCP1;Km^r	This study
χM1502	RS218 *zgf-1*::Tn*10*dKanRCP1;Km^r	This study
χM1503	RS218 *zgh-1*::Tn*10*dKanRCP1;Km^r	This study
χM1504	RS218 *zha-1*::Tn*10*dKanRCP1;Km^r	This study
χM1505	RS218 *zhd-1*::Tn*10*dKanRCP1;Km^r	This study
χM1506	RS218 *zhf-2*::Tn*10*dCamMCS;Cm^r	This study
χM1507	RS218 *zid-1*::Tn*10*dKanRCP1;Km^r	This study
χM1508	RS218 *zie-1*:Tn*10*dKanRCP1;Km^r	This study
χM1509	RS218 *zif-1*::Tn*10*dKanRCP1;Km^r	This study
Phage		
P1Δ*dam rev6*	Large plaque revertant of P1 cm *c*1.100 r^- m^- *dam*ΔMB	D. Friedman (31)
Plasmid		
pGI250	Suicide vector for delivery of Tn*10*dKanRCP1; Km^r Em^r *tac* promoter-inducible altered-target-specificity transposase	J. Mahillon (13)

[a] The insertion in strain χM1342, in contrast to those in the eight other minitransposon insertion mutants of K-12 strains (see text), contained the Tn*10*dCamMCS element. The pool of inserts from which it was isolated was generated in GE2515 as described elsewhere (10).

fragment length (RFL) analyses by rearrangements or by base pair-level divergence. Nevertheless, more than half of the inserts introduced into the two strains caused *Not*I RFL isomorphisms. Pairs of MG1655 and RS218 *Not*I fragments with indistinguishable lengths were generated by the inserts at 70, 72, 75, 84, and 85 min (Table 2 [χM1349 and χM1504; χM1350 and χM1505; χM1352 and χM1506; χM1354 and χM1508; and χM1355 and χM1509]; Fig. 1A, lanes 6 and 7; Fig. 1B, lanes 6 and 7 and 8 and 9).

A comparative *Not*I restriction map of strains MG1655 and RS218 between 63 and 86 min was made by aligning the native *Not*I fragments from the two strains at the integration sites of pairs of corresponding Tn*10*dKanRCP1 inserts (i.e., by aligning the native fragments with genetic clamps [Fig. 1C]) and then comparing the lengths of the corresponding subfragments from the two strains. This process indicated that in all of the instances of RFL isomorphism described above, a shared endpoint of each isomorphic *Not*I fragment pair was generated

TABLE 2. Minitransposon Tn*10*dKanRCP1-mediated *Not*I cleavages

Tn*10*dKanRCP1 insert-bearing strain[a]	Disrupted native fragment (kb)[b]	Lengths (kb) of subfragments (CW, CCW)[c]	Linkage map coordinate of Tn*10*dKanRCP insert (min)[d]
χM1346	A_{MG655} (992)	750, 240	63
χM1501	A_{RS218} (870)	795, 75	
χM1347	A_{MG1655} (992)	650, 340	65
χM1502	A_{RS218} (870)	660, 175[e]	
χM1348	A_{MG1655} (992)	540, 450	67
χM1503	A_{RS218} (870)	530, 340	
χM1349	A_{MG1655} (992)	**420**, 570	70
χM1504	A_{RS218} (870)	**420**, 450	
χM1350	A_{MG1655} (992)	**360**, 630	72
χM1505	A_{RS218} (870)	**360**, 510	
χM1352	A_{MG1655} (992)	**230**, 760	75
χM1506	A_{RS218} (870)	**230**, 640	
χM1353	L_{MG1655} (207)	139, 68	83
χM1507	K_{RS218} (178)	131, 47	
χM1354	L_{MG1655} (207)	**78**, 129	84
χM1508	K_{RS218} (178)	**78**, 100	
χM1355	L_{MG1655} (207)	**52**, 155	85
χM1509	K_{RS218} (178)	**52**, 126	

[a] The insertions in strains χM1352 and χM1506 were generated with Tn*10*dCamMCS (10) instead of Tn*10*dKanRCP1.

[b] Fragments are labeled as in the legend to Fig. 1.

[c] Pulsed-field gel electrophoresis pulse ramping over ranges determined according to the equation described by Smith (4) was used for resolution and/or sizing of particular fragments. Fragment sizes were interpolated as described elsewhere (10). Fragment pairs were considered to be isomorphic (shown in boldface) if they were indistinguishable after side-by-side electrophoresis with appropriately targeted pulse ramping for 12 h. Values show physical map orientations (clockwise [CW] or counterclockwise [CCW], according to the convention for *E. coli* K-12 [2]) as indicated by the *Not*I digestion patterns of the genomic DNAs from strains bearing insertions at neighboring linkage map coordinates contained by the same native fragment (see text) (and by the *Not*I digestion patterns of genomic DNAs from double insertion mutants generated by transduction of strain χM1506 with lysates of strains χM1502, χM1503, χM1504, and χM1505).

[d] According to the convention for *E. coli* K-12 (19, 28).

[e] The full-length RS218 subfragment counterclockwise of the 65-min insert was expected to be 210 kb (see Fig. 1).

by one of two conserved preexisting *Not*I sites (at either 81 or 86 min) and that, therefore, the respective subfragments forming each isomorphic pair contain corresponding chromosomal segments. Moreover, the map indicated that all of the isomorphic pairs themselves are nested in relation to one or the other of the conserved *Not*I sites. Thus, the longest isomorphic pair in each of the two nested series, which together account for more than half (996 of 1,930 kb) of the MG1655 and RS218 sequences between ~63 and ~86 min, appeared to contain conserved ordered arrays of shared homologies (i.e., of Tn*10*dKanRCP1 insert integration sites) that are uninterrupted by insertions or deletions.

The high proportion of *Not*I RFL isomorphisms detected between strains MG1655 and RS218 could be understood as a function of both (i) conservation of gene order between *E. coli* strains (cf. reference 25) and (ii) conservation of coinherited *Not*I sites in DNAs that are diverged at only ~3% of base pair positions (as are, generally, the chromosomal DNAs from random *E. coli* isolates [16]). This isomorphism served as a baseline for comparisons with which it was possible to detect localized RFL discrepancies between the two strains. Indeed, the *Not*I RFL polymorphism in the 63- to 86-min region of the MG1655-RS218 comparative map was fully accounted for by just a few segments of RFL dimorphism (explainable as insertions or deletions) interposed between isomorphic segments (Fig. 1C).

Evidence for strain-specific DNA additions or deletions in the chromosomal region from 63 to 86 min was obtained as *Not*I RFL dimorphisms between MG1655 and RS218 DNAs or as a shortened RS218 *Not*I subfragment (generated by strain RS218's incorporation of the 65-min chromosomal landmark) (Fig. 1C). Five DNA bulges (or loops [20]) were indicated in this region of the comparative map; two contained excess RS218 DNAs (55 of 973 kb [~6%]), and three contained excess MG1655 DNAs (39 of 957 kb [~4%]). The bulges detected by this method possibly represented insertions of chromosomal sequences unique to each strain. At least one of them, the RS218 bulge at 65 min, contained a strain-specific virulence gene cluster that is widely thought to have originated by interspecies gene transfer (4a). Also, the possibility that some of them represented deletions or duplications or rearrangements involving sequences from outside the mapped interval could not be excluded. Detection of isomorphisms and only five localized dimorphisms raises the heretofore unrecognized possibility that extensive RFL isomorphisms may exist generally between the chromosomal DNAs of evolutionarily diverged *E. coli* isolates and that these might be masked (in native macrorestriction digestion patterns) by a relatively few genetic events.

The analysis of diverged *E. coli* chromosomes by use of Tn*10*dKanRCP1 insertion alleles (mobile physical map landmarks) was reminiscent of heteroduplex analysis of bacteriophage DNAs, in that the latter procedure also yields structures composed of subunits that can be classed as either nearly identical or substantially unrelated (32). However, a much lower density of association points between the diverged DNAs was achieved by the present method. Because of this, chromosomal intervals that were found to contain dimorphisms may contain significant domains of sequence similarity as well, while DNA segments identified as similar by their RFL isomorphism are also undoubtedly diverged, at least at the level of base pair substitutions.

The method for comparative genome mapping reported here is theoretically applicable to any *E. coli* strain that is susceptible to generalized transduction with P1. Moreover, this comparative strategy may be used to characterize physical map degeneracy in other species under virtually any circumstances in which gene order is conserved and the fidelity of allelic exchanges can be maintained. It is anticipated that through comparisons across three or more *E. coli* lineages it will generally be possible to infer whether the chromosomal structure forming one half of any given RFL dimorphism is derived or ancestral (and thus whether derived forms arose by DNA additions or deletions). This may supplement the unrooted *E. coli* genetic trees that have been determined by multilocus enzyme electrophoretotyping (26) and permit inferences about the contribution of chromosomal additions or deletions to the evolution of lineages (see below).

An efficient feature of the method demonstrated here is that by this approach it is unnecessary to construct complete chromosome maps before comparing particular chromosomal intervals. In this respect, the method is analogous to PCR-based sequencing comparisons between isolates from divergent lineages (14). This is because in both instances corresponding intervals defined by flanking sites of shared homology (detected with Tn*10*dKanRCP1 insertions or with PCR primers, respectively) are targeted for comparison. Although comparative macrorestriction mapping with mobile physical map landmarks fails to distinguish the base pair substitutions detectable by sequencing, a significant advantage is that it allows

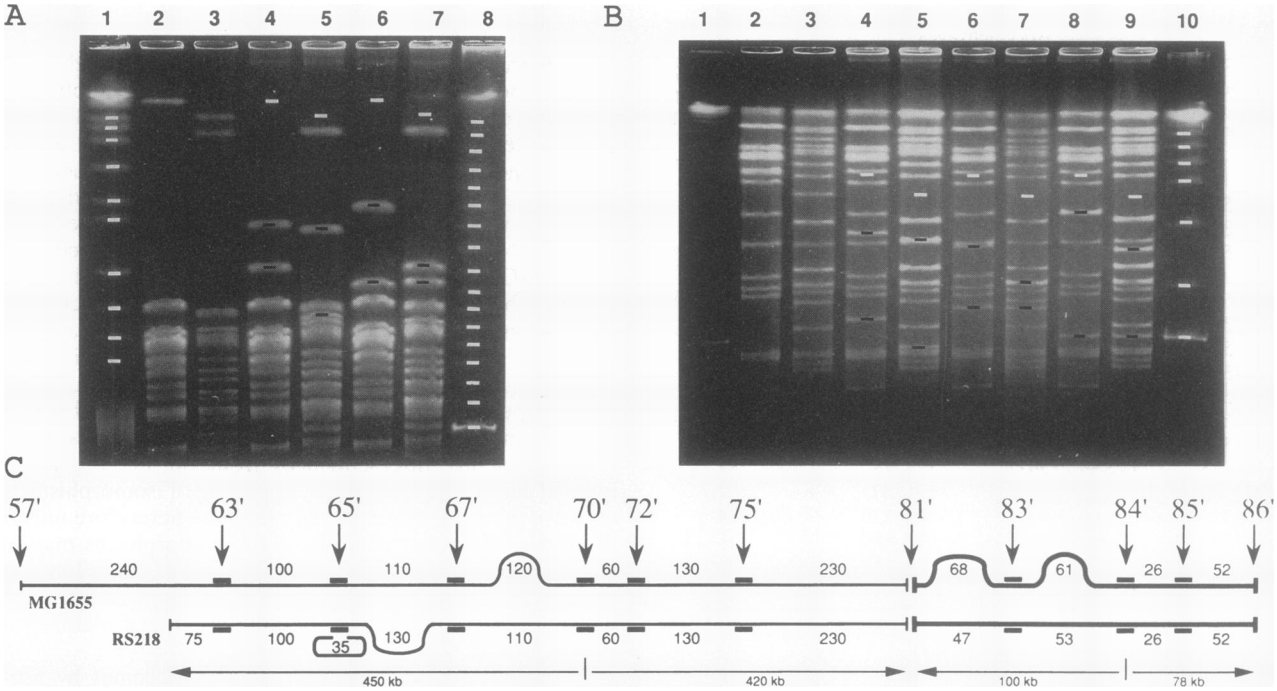

FIG. 1. Comparative macrorestriction mapping between 63 and 86 min with mobile physical map landmarks. (A) *Not*I restriction mapping of chromosomal landmarks between 63 and 81 min inherited as Tn*10*dKanRCP1 inserts by MG1655 and RS218 transductants. Pulsed-field gel electrophoresis pulse ramping was from 35 to 40 s for 9.5 h and from 55 to 60 s for 14.5 h. Lanes: 1, yeast chromosomes (Bethesda Research Laboratories, Bethesda, Md.); 2, MG1655; 3, RS218; 4, χM1348; 5, χM1503; 6, χM1349; 7, χM1504; 8, λ concatemers (Bethesda Research Laboratories). (Lane pairs 4 and 5 and 6 and 7 were of MG1655 and RS218 transductants containing pairs of corresponding chromosomal landmarks near 67 and 70 min, respectively.) Yeast chromosomes were as follows (marked at left by white bars), in order of ascending sizes: 0.21, 0.28, 0.35, 0.44, 0.55, 0.60, 0.68, 0.75, 0.79, and 0.83 mb. λ concatemers were as follows (marked at right), in order of ascending sizes: 48.5, 97, 145.5, 194, 242.5, 291, 339.5, 388, 436.5, 485, 533.5, 582, 630.5, 679, 727.5, 776, and 824.5 kb. The 22 native *Not*I fragments from MG1655 genomic DNA, with lettering and sizes (kilobases) according to Heath et al. (10), were as follows: A, 992; B, 358; C, 358; D, 279; E, 263; F, 251; G, 273; H, 245; I, 90; J, 214; K, 153; L, 207; M, 190; N, 129; O, 251; P, 103; R, 96; S, 36; T, 38; U, 41; V, 14; and W, 14. (Note that band Q, representing the F factor in K-12 strain EMG2 [29], is missing from the MG1655 digest [1].) Fragment A_{RS218} (870 kb) was the uppermost band in RS218's *Not*I digest pattern. The positions of new fragments (two per lane) and missing parental fragments (one per lane) in the *Not*I digests of the transductants' DNAs are marked by black bars and white bars, respectively. (B) *Not*I restriction mapping of chromosomal landmarks between 81 and 86 min. PFGE pulse ramping was from 8 to 10 s over 16 h and from 21 to 22 s over 6 h. Lanes: 1, λ concatemers; 2, MG1655; 3, RS218; 4, χM1353; 5, χM1507; 6, χM1354; 7, χM1508; 8, χM1355; 9, χM1509; 10, λ concatemers. (Lane pairs 4 and 5, 6 and 7, and 8 and 9 were of MG1655 and RS218 transductants containing pairs of corresponding chromosomal landmarks near 83, 84, and 85 min, respectively.) λ concatemers (marked at left) and the *Not*I fragments from MG1655 were as described for panel A. Fragment K_{RS218} (178 kb) was the 11th band from the top in RS218's *Not*I digestion pattern. The changes in *Not*I digestion patterns inherited by the transductants are indicated as described for panel A. (C) Alignment of *Not*I restriction fragments with pairs of corresponding Tn*10*dKanRCP1 inserts (genetic clamps). The alignments indicated were based on genetic clamps near 63, 65, 67, 70, 72, 75, 83, 84, and 85 min (Table 2) and *E. coli* linkage map conservation. Double arrows extending from the RS218 landmarks near 70 and 84 min indicate the contributions of the data from Table 2, χM1504 and χM1508, respectively, to assembly of the map. The isomorphism depicted for the 63- to 65-min interval is speculative because of the absence of direct evidence of either RFL isomorphism or dimorphism for this segment. The RS218 bulge depicted at 65 min was linked by P1 transduction to the site of the 65-min Tn*10*dKanRCP1 insert in one-third of the transductants and mapped counterclockwise to this insert.

rapid detection of additions or deletions in chromosomal segments of much greater sizes (~10^2 to ~10^3 kb) than those readily screened by sequencing.

Rare-cutter restriction sites in naturally occurring transposable elements have been used to map large DNAs (30). In addition, the rare-cutter sites contained by the Tn*10* insertions in a *Salmonella typhimurium*::Tn*10* mapping set (24) have recently been used to facilitate physical mapping of related strains (11a, 12). However, limitations to the use of wild-type Tn*10* inserts for comparative mapping are that they retain the ability to transpose to new sites during transduction (11) as well as to cause chromosomal inversions, duplications, and deletions (21). These events might complicate interpretation of chromosomal landmarks, especially when divergence between strains may reduce the rate of incorporation of markers by homologous recombination (7).

Comparative genome mapping with genetically transmissible physical markers permits a bridging of the gulf between classical bacterial-genetics inference, which is generally confined to crosses between isogenic strains (cf. references 6 and 7), and molecular techniques that allow sequence-based inferences regardless of the possibilities for genetic analysis. Thus, application of this method (in addition to allowing rapid restriction mapping in uncharacterized strains) may result in evidence of chromosomal additions or deletions that can be both invisible to linkage analyses (cf. reference 22) and difficult to detect by nongenetic approaches to aligning diverged restriction fragments. Indeed, the method may be useful for mapping many of the lineage-specific traits (e.g., virulence factors) carried by different *E. coli* strains, provided the genes for those traits are contained in lineage-specific chromosomal insertions.

However, this method also represents a new approach to genealogy. This is because it provides not only an efficient way to distinguish chromosomal genotypes, as do both multilocus enzyme electrophoretotyping and classical serotyping, but also new markers of chromosomal genotype (additions or deletions) identified by a procedure that is independent of their phenotypes. (In contrast, the base pair substitutions in conserved genes identified by multilocus enzyme electrophoretotyping are strongly biased in favor of selective neutrality, and similarly, the sequence differences accounting for surface structure variation identified by their affects on serotype are strongly biased in favor of niche-specific selectivity.) Since the chromosomal additions or deletions identified by this procedure may theoretically be neutral or subject to natural selection, their phenotypes in actual cases can inform us about the role these events play in the evolution of adaptive variation.

We thank N. Kleckner, J. Mahillon, and N. Sternberg for materials and manuscripts prior to publication; G. Weinstock for technical advice; D. Clewell, S. Falkow, D. Kaiser, E. Radany, and an anonoymous reviewer for helpful suggestions; and Max and Regula Gysin for gracious accommodations at Valbella, Switzerland, during preparation of the manuscript.

This work was supported by Public Health Service FIRST award AI31419 (C.A.B.) from the NIAID and by NICHD grant HD28820 (Department of Pediatrics, University of Michigan).

REFERENCES

1. **Bachmann, B. J.** 1987. Derivations and genotypes of some mutant derivatives of *Escherichia coli* K-12, p. 1190–1219. *In* F. C. Neidhardt, J. L. Ingraham, K. B. Low, B. Magasanik, M. Schaechter, and H. E. Umbarger (ed.), *Escherichia coli* and *Salmonella typhimurium*: cellular and molecular biology, vol. 2. American Society for Microbiology, Washington, D.C.
2. **Bachmann, B. J.** 1990. Linkage map of *Escherichia coli* K-12, edition 8. Microbiol. Rev. **54:**130–197.
3. **Bender, J., and N. Kleckner.** 1992. IS*10* transposase mutations that specifically alter target site recognition. EMBO J. **11:**741–750.
4. **Birren, B., and E. Lai.** 1993. Pulsed field gel electrophoresis: a practical guide. Academic Press, Inc., San Diego, Calif.

4a. **Bloch, C. A., and C. R. Rode.** Unpublished data.

5. **Bloch, C. A., G. M. Thorne, and F. M. Ausubel.** 1989. General method for site-directed mutagenesis in *Escherichia coli* O18ac:K1:H7: deletion of the inducible superoxide dismutase gene, *sodA*, does not diminish bacteremia in neonatal rats. Infect. Immun. **57:**2141–2148.
6. **Demerec, M., A. G. Adelberg, A. J. Clark, and P. E. Hartman.** 1966. A proposal for a uniform nomenclature in bacterial genetics. Genetics **54:**61–76.
7. **Demerec, M., and N. Ohta.** 1964. Genetic analyses of *Salmonella typhimurium* × *Escherichia coli* hybrids. Proc. Natl. Acad. Sci. USA **52:**317–323.
8. **Dower, W. J., J. F. Miller, and C. W. Ragsdale.** 1988. High efficiency transformation of *E. coli* by high voltage electroporation. Nucleic Acids Res. **16:**6127–6145.
9. **Guyer, M. S., R. R. Reed, J. A. Steitz, and K. B. Low.** 1980. Identification of a sex-factor-affinity site in *E. coli* as γδ. Cold Spring Harbor Symp. Quant. Biol. **45:**135–140.
10. **Heath, J. D., J. D. Perkins, B. Sharma, and G. M. Weinstock.** 1992. *Not*I genomic cleavage map of *Escherichia coli* K-12 strain MG1655. J. Bacteriol. **174:**558–567.
11. **Kleckner, N., D. F. Barker, D. G. Ross, and D. Botstein.** 1978. Properties of the translocatable tetracycline-resistance element Tn*10* in *Escherichia coli* and bacteriophage lambda. Genetics **90:**427–450.

11a. **Liu, S.-L., A. Hessel, H.-Y. M. Cheng, and K. E. Sanderson.** 1994. The *Xba*I-*Bln*I-*Ceu*I genomic cleavage map of *Salmonella paratyphi* B. J. Bacteriol. **176:**1014–1024.

12. **Liu, S.-L., A. Hessel, and K. E. Sanderson.** 1993. The *Xba*I-*Bln*I-*Ceu*I genomic cleavage map of *Salmonella enteritidis* shows an inversion relative to *Salmonella typhimurium* LT2. Mol. Microbiol. **10:**655–664.
13. **Mahillon, J., and N. Kleckner.** 1992. New IS*10* transposition vectors based on a gram-positive replication origin. Gene **116:**69–74.
14. **Milkman, R., and M. K. Bridges.** 1993. Molecular evolution of the *Escherichia coli* chromosome. IV. Sequence comparisons. Genetics **133:**455–468.
15. **Miller, J. H.** 1992. A short course in bacterial genetics: a laboratory manual and handbook for *Escherichia coli* and related bacteria, p. 277–278, 357–364, 439–440. Cold Spring Harbor Laboratory Press, Cold Spring Harbor, N.Y.
16. **Nelson, K., and R. K. Selander.** 1992. Evolutionary genetics of the proline permease gene (*putP*) and the control region of the proline utilization operon in populations of *Salmonella* and *Escherichia coli*. J. Bacteriol. **174:**6886–6895.
17. **Okada, N., C. Sasakawa, T. Tobe, K. A. Talukder, K. Komatsu, and M. Yoshikawa.** 1991. Construction of a physical map of the chromosome of *Shigella flexneri* 2a and the direct assignment of nine virulence-associated loci identified by Tn*5* insertions. Mol. Microbiol. **5:**2171–2180.
18. **Perkins, J. D., J. D. Heath, B. R. Sharma, and G. M. Weinstock.** 1992. *Sfi*I genomic cleavage map of *Escherichia coli* K-12 strain MG1655. Nucleic Acids Res. **20:**1129–1137.
19. **Perkins, J. D., J. D. Heath, B. R. Sharma, and G. M. Weinstock.** 1993. *Xba*I and *Bln*I genomic cleavage maps of *Escherichia coli* K-12 strain MG1655 and comparative analysis of other strains. J. Mol. Biol. **232:**419–445.
20. **Riley, M., and K. E. Sanderson.** 1990. Comparative genetics of *Escherichia coli* and *Salmonella typhimurium*, p. 85–96. *In* K. Drlica and M. Riley (ed.), The bacterial chromosome. American Society for Microbiology, Washington, D.C.
21. **Ross, D., J. Swan, and N. Kleckner.** 1979. Physical structures of Tn*10*-promoted deletions and inversions: role of 1400 base pair inverted repetitions. Cell **16:**721–731.
22. **Rothman, S. J. L.** 1965. Transduction studies on the relation between prophage and host chromosome. J. Mol. Biol. **12:**892–912.
23. **Russell, K. Y., C. K. Rode, and C. A. Bloch.** 1993. Recombination-based approach to physical mapping of neonatal-sepsis-associated *Escherichia coli*, abstr. H-56, p. 200. Abstr. 93rd Annu. Meet. Am. Soc. Microbiol. 1993. American Society for Microbiology, Washington, D.C.
24. **Sanderson, K. E., and J. R. Roth.** 1988. Linkage map of *Salmonella typhimurium*, edition VII. Microbiol. Rev. **52:**485–532.
25. **Segall, A., M. J. Mahan, and J. R. Roth.** 1988. Rearrangement of the bacterial chromosome: forbidden inversions. Science **241:**1314–1318.
26. **Selander, R. K., D. A. Caugant, and T. S. Whittam.** 1987. Genetic structure and variation in natural populations of *Escherichia coli*, p. 1625–1647. *In* F. C. Neidhardt, J. L. Ingraham, K. B. Low, B. Magasanik, M. Schaechter, and H. E. Umbarger (ed.), *Escherichia coli* and *Salmonella typhimurium*: cellular and molecular biology, vol. 2. American Society for Microbiology, Washington, D.C.
27. **Silver, R. P., W. Aaronson, A. Sutton, and R. Schneerson.** 1980. Comparative analysis of plasmids and some metabolic characteristics of *Escherichia coli* K1 from diseased and healthy individuals. Infect. Immun. **29:**200–206.
28. **Singer, M., T. A. Baker, G. Schnitzler, S. M. Deischel, M. Goel, W. Dove, K. J. Jaacks, A. D. Grossman, J. W. Erickson, and C. M. Gross.** 1989. A collection of strains containing genetically linked alternating antibiotic resistance elements for genetic mapping of *Escherichia coli*. Microbiol. Rev. **53:**1–24.
29. **Smith, C. L., J. G. Econome, A. Schutt, S. Klco, and C. R. Cantor.** 1987. A physical map of the *Escherichia coli* K12 genome. Science **236:**1448–1453.
30. **Smith, C. L., and R. D. Kolodner.** 1988. Mapping of *Escherichia coli* chromosomal Tn*5* and F insertions by pulsed field gel electrophoresis. Genetics **119:**227–236.
31. **Sternberg, N. L., and R. Maurer.** 1991. Bacteriophage-mediated generalized transduction in *Escherichia coli* and *Salmonella typhimurium*. Methods Enzymol. **204:**18–43.
32. **Westmoreland, B. C., W. Szybalski, and H. Ris.** 1968. Mapping deletions and substitutions in heteroduplex DNA molecules of bacteriophage Lambda by electron microscopy. Science **163:**1343–1348.